Analytical and Bioanalytical Chemistry (2022) 414:7957–7965
https://doi.org/10.1007/s00216-022-04333-8

PAPER IN FOREFRONT

COVID-19 variants' cross-reactivity on the paper microfluidic particle counting immunoassay

Sangsik Kim[1] · Ciara Eades[2] · Jeong-Yeol Yoon[1]

Received: 29 July 2022 / Revised: 31 August 2022 / Accepted: 7 September 2022 / Published online: 21 September 2022

Abstract

SARS-CoV-2 has mutated many times since the onset of the COVID-19 pandemic, and the omicron is currently the most dominant variant. Determining the specific strain of the virus is beneficial in providing proper care and containment of the disease. We have previously reported a novel method of counting the number of particle immunoagglutination on a paper microfluidic chip using a smartphone-based fluorescence microscope. A single-copy-level detection was demonstrated from clinical saline gargle samples. In this work, we further evaluated two different SARS-CoV-2 monoclonal antibodies to spike vs. nucleocapsid antigens for detecting omicron vs. delta and spike vs. nucleocapsid proteins. The SARS-CoV-2 monoclonal antibody to nucleocapsid proteins could distinguish omicron from delta variants and nucleocapsid from spike proteins. However, such distinction could not be found with the monoclonal antibody to spike proteins, despite the numerous mutations found in spike proteins among variants. This result may suggest a clue to the role of nucleocapsid proteins in recognizing different variants.

Keywords COVID-19 · Omicron · Delta · Cross-reactivity · Smartphone microscope · Paper microfluidic chip

Introduction

SARS-CoV-2 has already mutated many times during the worldwide COVID-19 pandemic. World Health Organization (WHO) has identified the variants of concern (VOCs) into alpha (B.1.1.7), beta (B.1.351), gamma (P.1), delta (B.1.617.2), and omicron (B.1.1.529) [1]. In addition, there are six other variants of interests (VOI) as reported by WHO. The omicron variants have become dominant since December 2021. There are subvariants of omicron, from BA.1 through BA.5, and the BA.5 subvariant is the current dominant strain of COVID-19 worldwide [2]. The omicron variants have more than 60 mutations, with many mutations on their spike proteins. They are characterized by high transmissibility — the reproduction number is reported to be triple that of the delta variant [3]. While their symptoms are less severe, they still pose significant threats to unvaccinated, elderly, and people with underlying conditions [1].

Reverse transcription polymerase chain reaction (RT-PCR) has served as the de facto standard method of SARS-CoV-2 detection, initially from nasopharyngeal swabs, later from nasal swabs, and recently from saliva collection [4, 5]. Many countries are now adopting rapid antigen tests as the first line of detection [6] while using RT-PCR as the in-depth verification tool. More people are also relying on at-home antigen tests and choosing not to report to the government, which may lead to an incorrectly reduced number of new cases [7]. However, rapid antigen tests are substantially less accurate than RT-PCR, especially during the early phase of infections. In addition, they cannot differentiate the virus variants [6].

Many methods have been introduced to improve the accuracy and detection limit of rapid antigen tests. For example, our laboratory has recently used a smartphone-based fluorescence microscope on a paper microfluidic chip to demonstrate the single-copy-level detection of SARS-CoV-2 [8]. However, with the rapid introduction of new mutations, we must demonstrate the ability to identify different SARS-CoV-2 variants on these antigen tests. Identifying the variants on these assay platforms is

✉ Jeong-Yeol Yoon
jyyoon@arizona.edu

[1] Department of Biomedical Engineering, The University of Arizona, Tucson, AZ 85721, USA

[2] Department of Chemistry & Biochemistry, The University of Arizona, Tucson, AZ 85721, USA

crucial to determining the outcome of disease prevention and mitigation. It may also clarify whether a new vaccine is necessary for the newly identified variant by connecting the antibody used in the antigen test to the neutralizing antibodies formed from vaccination. For example, Su et al. investigated the cross-reactivity and cross-protection of an influenza vaccine against other subtypes [5]. Their vaccine (live attenuated virus) elicited an immune response against multiple virus forms. It emphasizes the importance of cross-reactivity to determine the vaccine's efficacy against the other subtypes of variants. The antibody's cross-reactivity (on an antigen test) can explain the effectiveness of a vaccine and determine the demand for a revised vaccine.

Our previous work [8] utilized antibody-conjugated fluorescent particles on a paper-based microfluidic chip for a sensitive SARS-CoV-2 assay. Clinical saline gargle samples were loaded onto the chip and left for a few minutes to induce particle aggregation from antibody-antigen binding (i.e., particle immunoagglutination). A smartphone-based fluorescence microscope counted the particle aggregation from the paper chip. Limit of detection (LOD) was below a single copy (1 fg) level, and the accuracy was 93% with $n = 27$ human clinical subjects (compared to RT-PCR results) [8]. Similar work has also been published using magnetic beads on a 96-well plate [9]. The smartphone detected the well plate's colorimetric signals to determine the viral load.

In this study, we repeated the experiments of Breshears et al. [8] to determine the reactivity of SARS-CoV-2 antibodies to delta and omicron variants. Delta and omicron antigens were spiked to human saline gargle samples, and the fluorescent particles conjugated with antibodies were used. Specifically, Breshears et al. demonstrated improved sensitivity using nucleocapsid antibodies rather than spike antibodies [8]. Since many SARS-CoV-2 mutations are found in spike antigens, nucleocapsid antibodies may induce substantial cross-reactivity. However, as shown in this work, the results were the other way round, which may provide a clue to the mechanism of cross-binding, at least for the particle counting immunoassay method demonstrated in this work.

Materials and methods

Antibodies and antigens

Two types of antibodies were purchased from Sino Biological (Beijing, China): SARS-CoV-2 spike neutralizing antibody (40,591-MM48; mouse monoclonal antibody) and SARS-CoV-2 nucleoprotein antibody (40,143-MM05; mouse monoclonal antibody). The manufacturer reported that both antibodies bind to all SARS-CoV-2 variants, including delta and omicron. These antibodies were covalently conjugated to yellow-green fluorescent carboxylated particles described in the following section. In addition, target antigens were also purchased from Sino Biological: omicron spike RBD protein (40,592-V08H121), omicron nucleocapsid protein (40,588-V07E34), delta spike S1 + S2 protein (40,589-V08B16), and delta nucleocapsid protein (40,588-V07E29).

Antibody conjugation to fluorescent polystyrene particles

The SARS-CoV-2 antibodies were covalently conjugated to the yellow-green fluorescent carboxylated polystyrene particles (diameter of 0.5 µm; CAYF500NM; Magsphere, Inc., Pasadena, CA, USA). The amine group in the antibody was utilized to form a covalent bond with the carboxyl group of the particles to form a peptide bond by carbodiimide chemistry. 1 mg/mL 1-ethyl-3-(3-dimethylaminopropyl)carbodiimide (EDAC; E7750; Sigma-Aldrich, St. Louis, MO) was added to the particle suspension to activate the particles and covalently crosslink the antibodies to the particles. 0.1 mg/mL bovine serum albumin (BSA; BP700100; Thermo Fisher Scientific, Waltham, MA) was used as a blocking agent to prevent nonspecific hydrophobic interactions between particles. The concentration of the particles was evaluated using the absorbance readings at 488 nm (excitation wavelength) and compared with the pre-determined standard curve. Particles were washed three times through centrifugation ($8{,}200 \times g$ for 1 min) and resuspension, to remove unreacted and excess molecules. In the final step, the antibody-conjugated particle suspension was sonicated for 10 min to minimize self-aggregation. The particle suspension was added with Tween 20 solution at the final concentrations of 0.02% (w/v) particles and 0.05% (v/v) Tween 20. Particles were stored at 4 °C in a refrigerator. Particles' self-aggregation was checked with a benchtop fluorescence microscope before the assays and sonicated for 10 min when needed. More details can be found in the previous works [8, 10].

Paper-based microfluidic chip

The paper-based microfluidic chips were printed the same way as in the previous work [8, 10]. ColorQube 8580 wax printer (Xerox, Norwalk, CT, USA) was used to print the channel designs, followed by heating on a hot plate to melt the printed wax through the depth of a paper. A single chip contained four dumbbell-shaped channels for conducting four different assays, where the dumbbell shapes at both ends acted as the adsorbent

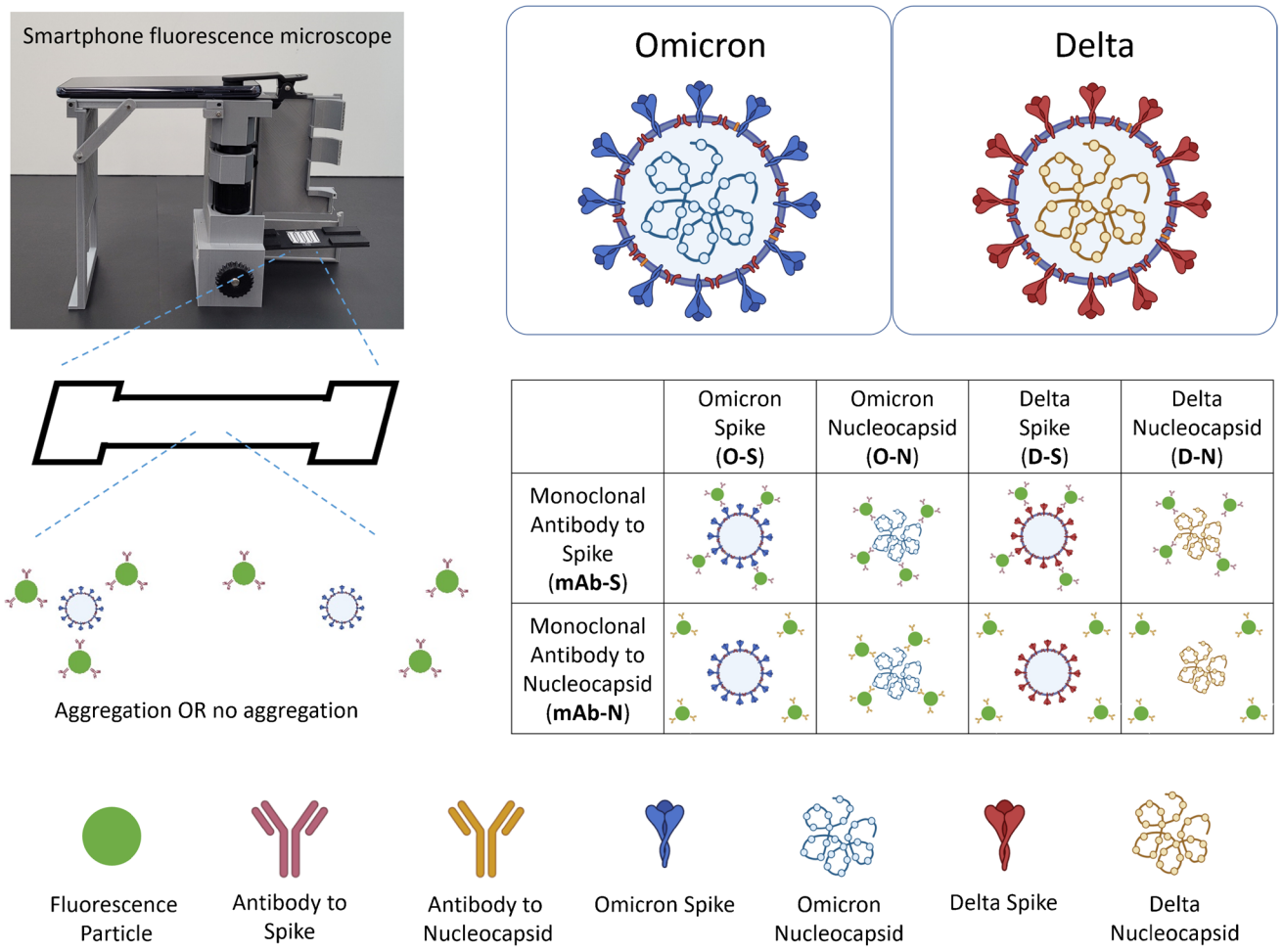

Fig. 1 The assay platform and the overall experimental design

pads. Nitrocellulose paper (FF80 HP Plus from GE Healthcare, Chicago, IL, USA) was used, whose capillary rise was 60–100 s per 4 cm, and the total caliper was 200 µm, according to the manufacturer.

Assay procedure

SARS-CoV-2 variant antigens were spiked to 10% human saliva (IRHUSL250mL, Innovative Research, Novi, MI, USA) diluted in 0.9% w/v sterile NaCl (Addipak®, Teleflex Medical, Research Triangle Park, NC, USA). These 10% saliva + 0.9% NaCl simulated clinical saline gargle samples [11]. Four microliters of the antigen-spiked saline sample was pipetted into the middle of the paper microfluidic chip. We then waited 10 min for the sample to spontaneously spread over the channel length through capillary action. After that, 4 µL of antibody-conjugated particle suspension was loaded to the center of the channel. An additional 5 min was needed for the antibody and antigen to interact and for the particles to aggregate.

Smartphone-based fluorescence imaging of the paper microfluidic chips

The smartphone-based fluorescence microscope, described in the previous research [8], was used to count the number of aggregated particles and evaluate the extent of antibody-antigen binding.

Image processing

The image processing was carried out following the method described in the previous research [8, 10]. All smartphone microscopic images were separated into red, green, and blue channels, and the green channel was analyzed. First, the pixels with an intensity less than 125 out of 255 were considered noise (autofluorescence of paper) and removed from the image. (The background noise was cloudy green with an average intensity of 99, while the particles were clear spherical circles with an average intensity of 161.) The images were then binarized.

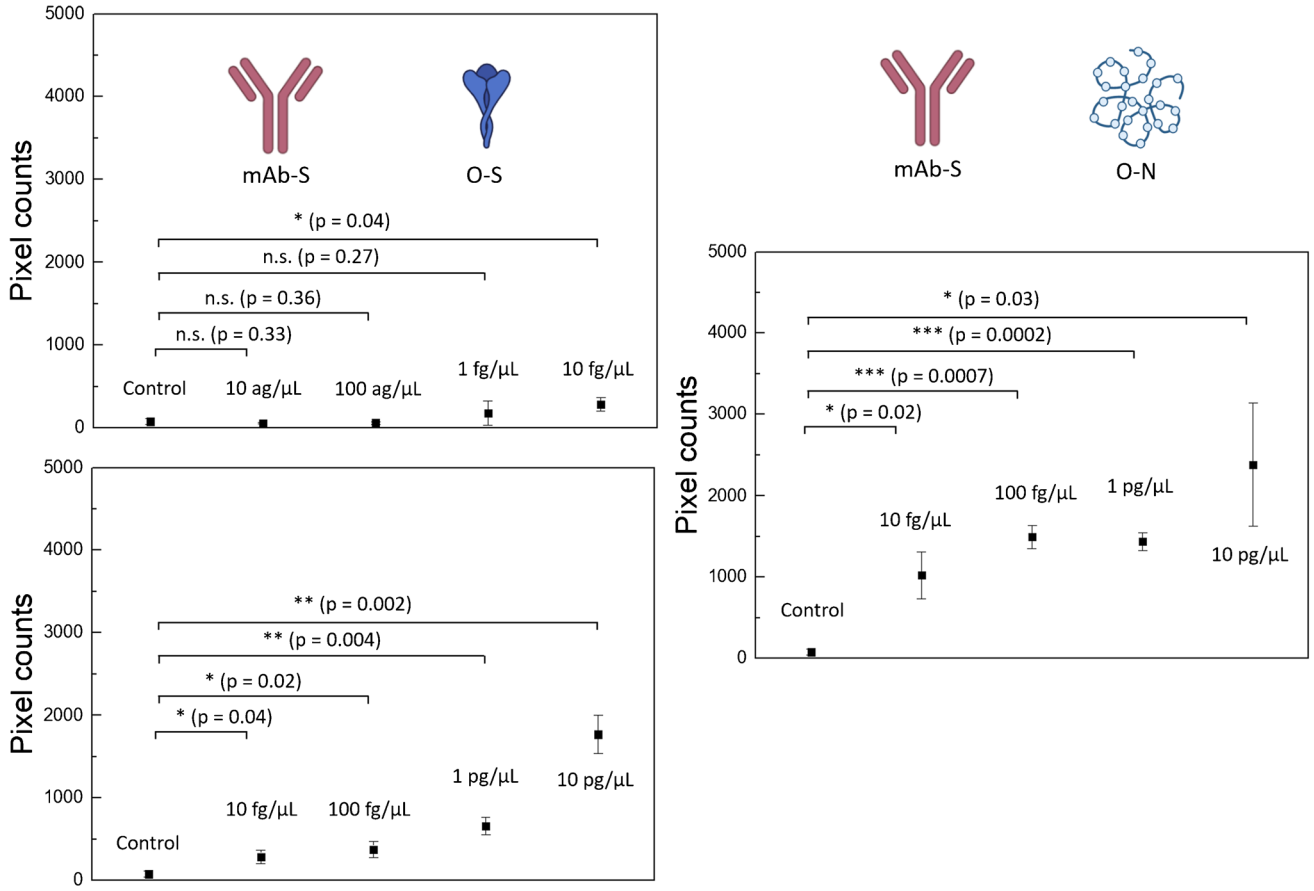

Fig. 2 The assay results of monoclonal antibody to SARS-CoV-2 spike proteins (mAb-S) to omicron spike (O-S) and omicron nucleocapsid (O-N) proteins, spiked to saline gargle samples (10% saliva with 0.9% NaCl). Average of four different experiments, each time on different channels. Error bars represent standard errors. * denotes $p \leq 0.05$; ** denotes $p \leq 0.01$; n.s. denotes not significant

The pixel areas of each "particle" were evaluated. The pixel areas < 21 were considered non-aggregated and removed, while those ≥ 21 were considered aggregated particles. The pixel counts of aggregated particles were added together for three images taken from a single paper microfluidic channel and used as a single data point for each channel. For a given set of antibody-antigen pair and a specific concentration, this set of experiments was repeated four times. All image processing was conducted using a custom MATLAB code (MathWorks; Natick, MA, USA). Further details were described in the previous research [8, 10].

Statistical analysis

All assay results (pixel counts) were compared with the control using a one-tailed *t*-test with unequal variances with Microsoft Excel. The *p* values were evaluated and those ≤ 0.05 were marked *, ≤ 0.01 marked **, ≤ 0.001 marked ***, ≤ 0.0001 marked ****, and > 0.05 marked n.s. (not significant).

Results

Two types of SARS-CoV-2 antibodies to spike and nucleocapsid proteins (mAb-S and mAb-N) were tested to detect four different SARS-CoV-2 antigens from simulated saline gargle samples. These include omicron spike (O-S), omicron nucleocapsid (O-N), delta spike (D-S), and delta nucleocapsid (D-N) proteins. Figure 1 shows the overall experimental design and the assay platforms.

A dumbbell-shaped paper microfluidic channel was used, where the antigen-spiked saline gargle samples (10% saliva with 0.9% NaCl) were loaded first to the center, followed by the antibody-conjugated fluorescent particle suspension also to the center. Solutions spread evenly to both sides of the channel via capillary action. The smartphone-based fluorescence microscope imaged the antibody-conjugated particles' aggregation resulting from antibody-antigen binding from each paper microfluidic channel [8]. Green channel images were collected, thresholded to remove the noises, and binarized. Pixel numbers were obtained from each particle cluster, and the small particle clusters were

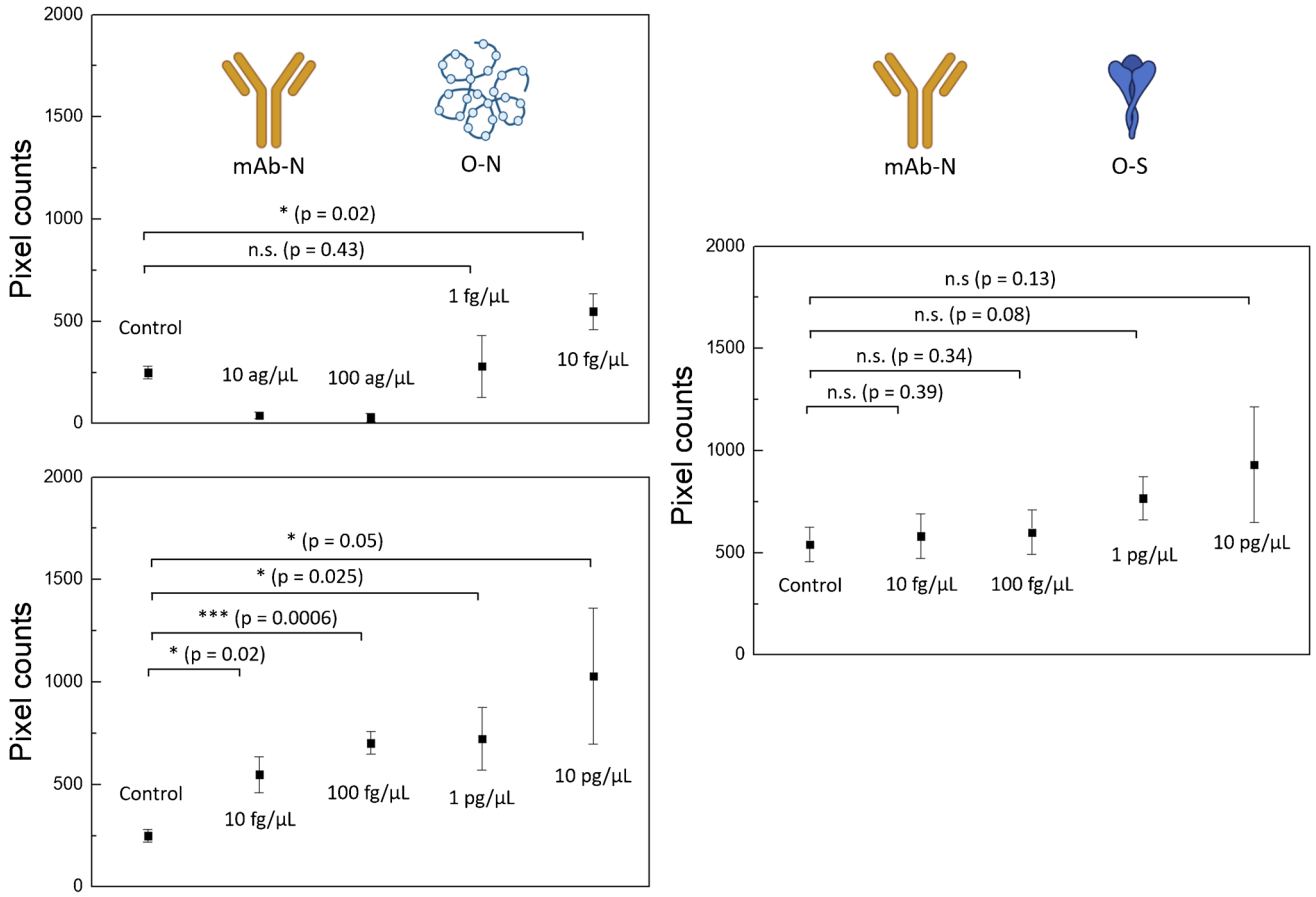

Fig. 3 The assay results of monoclonal antibody to SARS-CoV-2 nucleocapsid proteins (mAb-N) to omicron nucleocapsid (O-N) and omicron spike (O-S) proteins, spiked to saline gargle samples (10% saliva with 0.9% NaCl). Average of four different experiments, each time on different channels. Error bars represent standard errors. * denotes $p \leq 0.05$; *** denotes $p \leq 0.001$; n.s. denotes not significant

considered non-aggregated and removed. The pixel areas of "aggregated" particles were summed up for the entire image. Since three images were collected from a single channel, the total pixel areas were added together for three images. This number is then considered a single data for each channel. Such experiments were repeated four times to evaluate the averages and standard errors. The higher pixel counts correlated to the greater extent of particle aggregation and, subsequently, the higher number of antibody-antigen binding.

Figure 2 shows the results of monoclonal antibodies to SARS-CoV-2 spike proteins (mAb-S) to omicron spike (O-S) and omicron nucleocapsid (O-N) proteins. Since mAb-S and O-S are the correct pair, we conducted two different experiments with low-range concentrations (10 ag/μL to 10 fg/μL) and medium-range concentrations (10 fg/μL to 10 pg/μL). All concentrations at or above 10 fg/μL were significantly different ($p < 0.05$) from the negative control (non-SARS-CoV-2-spiked saline gargle samples), which is the LOD. To further lower the LOD, we added Tween 20 in all saline gargle samples. However, all pixel counts were attenuated, and the LOD was not improved. Considering the mass of a single SARS-CoV-2 particle of approximately 1 fg [8, 11] and the sample volume of 4 μL, 10 fg/μL is sufficiently close to the single virus copy level and significantly lower than the concentrations from the infected individuals [8, 11]. With mAb-S and O-N, however, higher pixel counts were also observed, with all concentrations significantly different from the negative control. This result indicates the mAb-S's ability to bind to O-N, despite not being a perfect match.

Experiments were repeated with monoclonal antibodies to SARS-CoV-2 nucleocapsid proteins (mAb-N) to O-S and O-N proteins. The results are shown in Fig. 3. The correct pair, mAb-N to O-N, behaved similarly to mAb-S to O-S (Fig. 2 on the left), with the LOD of 10 fg/μL. However, the incorrect pair, mAb-N to O-S, did not work. This result indicates the superior specificity of mAb-N (nucleocapsid antibody) over mAb-S (spike antibody) in distinguishing nucleocapsid (O-N) from spike (O-S) proteins.

Experiments were also conducted for mAb-S (spike antibody) to delta spike (D-S) and delta nucleocapsid (D-N) proteins. The results are shown in Fig. 4, which are like Fig. 2. The lower concentrations (10 ag/μL to

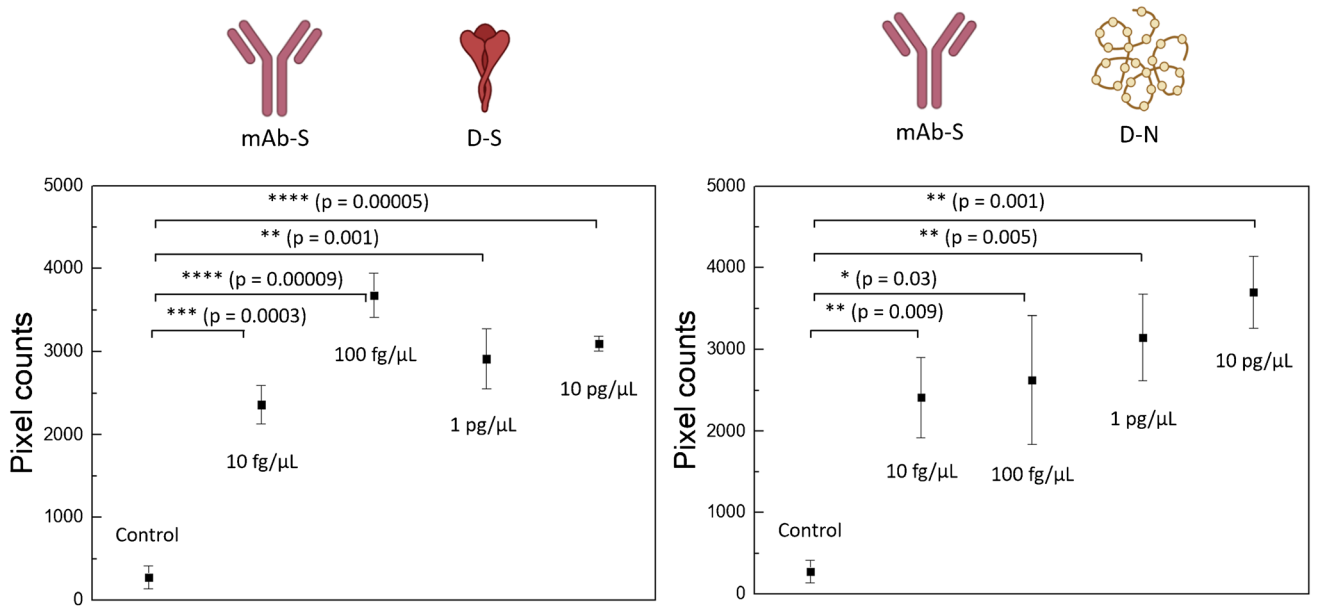

Fig. 4 The assay results of monoclonal antibody to SARS-CoV-2 spike proteins (mAb-S) to delta spike (D-S) and delta nucleocapsid (D-N) proteins, spiked to saline gargle samples (10% saliva with 0.9% NaCl). Average of four different experiments, each time on different channels. Error bars represent standard errors. * denotes $p \leq 0.05$; ** denotes $p \leq 0.01$; *** denotes $p \leq 0.001$; **** denotes $p \leq 0.0001$; n.s. denotes not significant

1 fg/μL) were not tested this time (as well as the results shown in Fig. 5), as they are not relevant to the clinical levels. The spike antibody (mAb-S) reacted to both antigens (D-S and D-N), even though D-N is not a perfect match. In addition, the overall pixel counts in Fig. 4 were substantially higher than those in Fig. 2, indicating the superior binding capability of mAb-S to delta antigens (over omicron antigens). While the LOD may be lower with delta antigens, we did not investigate further as it was not the focus of this work.

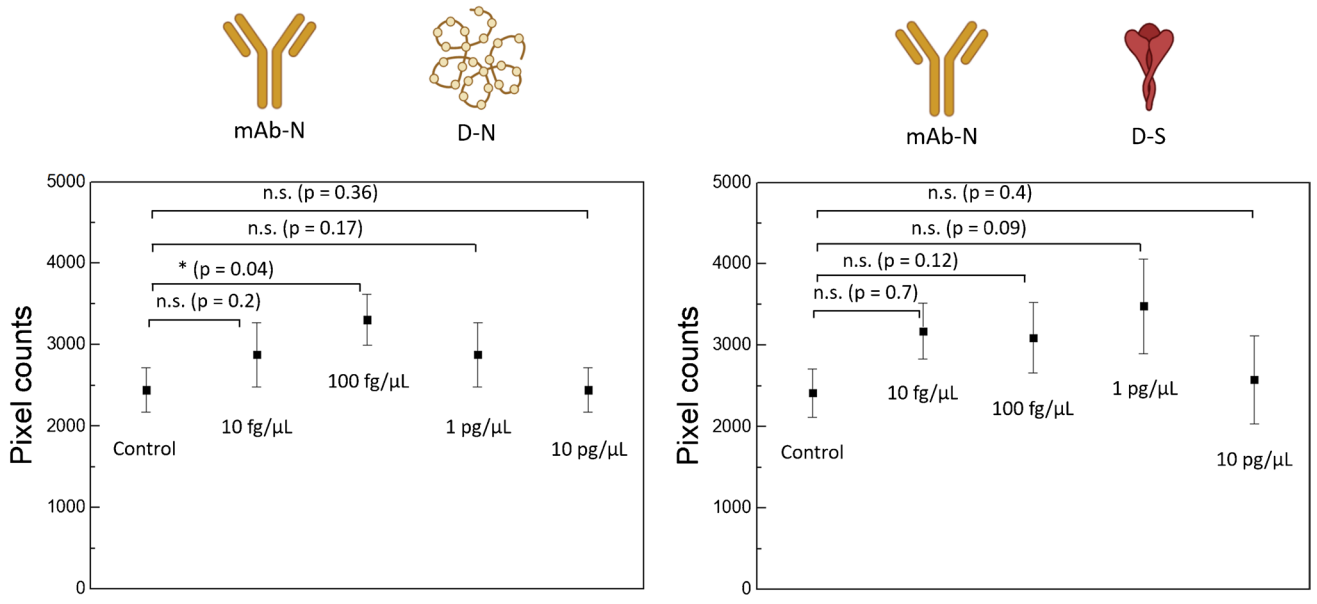

Fig. 5 The assay results of monoclonal antibody to SARS-CoV-2 spike proteins (mAb-S) to delta nucleocapsid (D-N) and delta spike (D-S) proteins, spiked to saline gargle samples (10% saliva with 0.9% NaCl). Average of four different experiments, each time on different channels. Error bars represent standard errors. * denotes $p \leq 0.05$; ** denotes $p \leq 0.01$; *** denotes $p \leq 0.001$; **** denotes $p \leq 0.0001$; n.s. denotes not significant

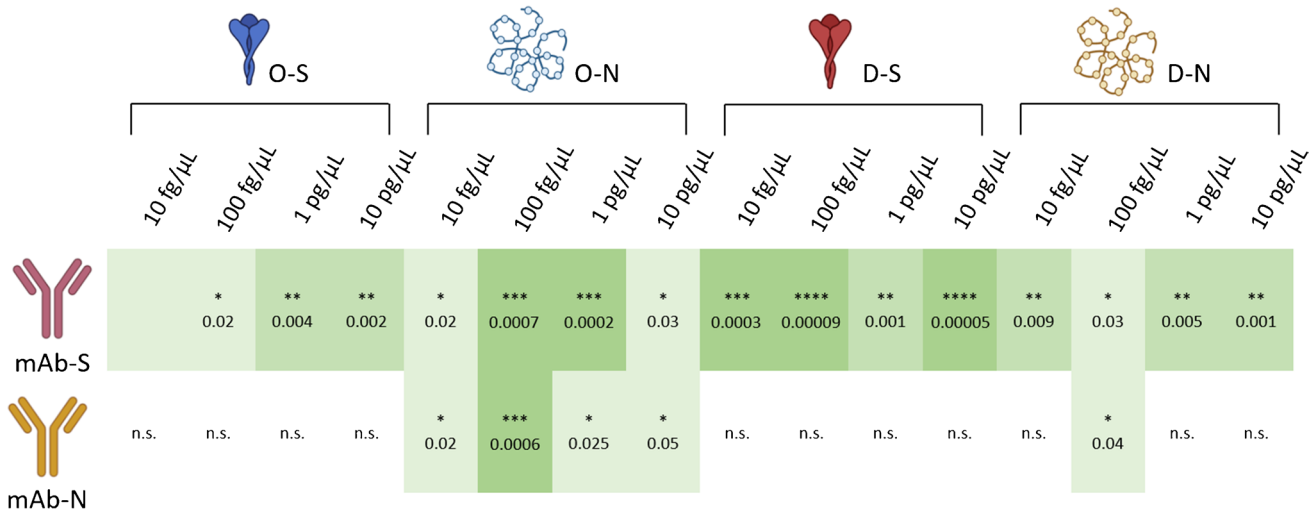

Fig. 6 The binding characteristics summary between spike vs. nucleocapsid antibodies to four antigens (spiked to the saline gargle samples) on a particle counting assay on a paper microfluidic chip with a smartphone-based fluorescence microscope

Finally, we conducted the experiments for mAb-N (nucleocapsid antibody) to delta nucleocapsid (D-N) and delta spike (D-S) proteins. The results are shown in Fig. 5. (The specific batch of antibody-conjugated particles was different for these experiments. The pixel counts were overall higher than those of Figs. 2, 3, and 4. They can be attributed to the higher particle concentration after the sonication and centrifuging processes. Since quantification is not the main focus of this work, we used the raw results without any attempt at normalization.) While the right pair (mAb-N to D-N) showed a significant difference at 100 fg/μL, all other concentrations were not significantly different from the negative control. Furthermore, the incorrect pair (mAb-N to D-S) showed no significant differences from the negative control.

Figure 6 summarizes all experiments. The spike antibody (mAb-S) binds to all four types of antigens, regardless of spike vs. nucleocapsid or omicron vs. delta. In contrast, the nucleocapsid antibody (mAb-N) binds only to omicron nucleocapsid proteins (O-N). This result suggests nucleocapsid antibodies' potential superiority in distinguishing between different variants.

Discussion

Two different SARS-CoV-2 monoclonal antibodies were used in this study — to spike (mAb-S) and nucleocapsid (mAb-N) proteins, respectively. Four antigen types were tested, omicron spike (O-S), omicron nucleocapsid (O-N), delta spike (D-S), and delta nucleocapsid (D-N). The spike antibodies (mAb-S) bind to all four antigen types. The binding of spike antibodies to the nucleocapsids has been reported in other viruses. Suomalainen et al. found that the spike-nucleocapsid interactions are required for disease spread and dissemination of alphavirus [12]. Additionally, the spike antibodies could bind to both omicron and delta antigens at similar extents. Such cross-binding could be explained by the presence of ACE2 receptor proteins in both omicron and delta variants. Han et al. analyzed the binding residues between the omicron and delta variants [13]. While some residues were mutated in the variants, the receptor protein (ACE2) maintained similar binding patterns with both strains. Critical binding residues of the hACE2 protein include H34, E35, Y83, F486, Q24, S19, Q42, D38, Y41, and K353 [13]. While the delta and omicron strains have slightly different binding abilities to the receptor protein, all these key residues are utilized in both scenarios.

On the other hand, the nucleocapsid antibodies (mAb-N) bind to omicron nucleocapsid (O-N) but not to the other antigen types. As mentioned earlier, the differences among SARS-CoV-2 variants could be found primarily in their spike proteins. Ye et al. showed that the nucleocapsid proteins were similar among the SARS-CoV-2 variants [14]. Despite this, the nucleocapsid antibodies could preferentially bind to omicron nucleocapsid but not to the other three types. The manufacturer reported the cross-reactivity to all five VOCs for both antibodies used in this work [15, 16]. Our previous work [8] found that the nucleocapsid antibody provided better clinical sensitivity than the spike antibody. We believe a similar scenario could be applied in distinguishing between omicron and delta variants.

To further evaluate such analytical specificity, we conducted a set of experiments using the polyclonal antibody to nucleocapsid protein (pAb-N) and the omicron nucleocapsid (O-N) spiked saline gargle samples. The results are shown in Fig. 7 on the left. Unlike the results with

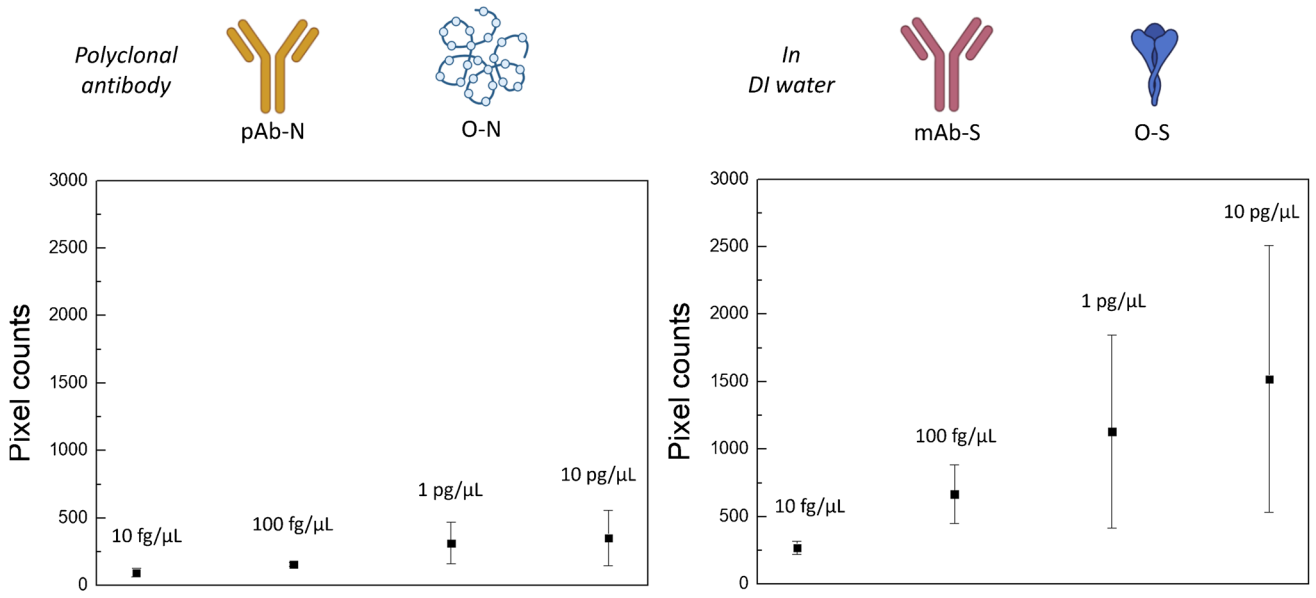

Fig. 7 Control experiments. Left: the assay results of polyclonal antibody to SARS-CoV-2 nucleocapsid proteins (pAb-N) to omicron nucleocapsid (O-N) proteins, spiked to saline gargle samples (10% saliva with 0.9% NaCl). Right: the assay results of monoclonal antibody to SARS-CoV-2 spike proteins (mAb-S) to omicron spike (O-S) proteins in DI water. Average of four different experiments, each time on different channels. Error bars represent standard errors

mAb-N, no significance could be observed for all concentrations, potentially indicating the analytical specificity of monoclonal antibodies.

Finally, we conducted another set of experiments with mAb-S and O-S in DI water. Neither saliva nor saline was used. As the concentration increased from 10 fg/μL to 10 pg/μL, the pixel count increased as expected. However, the standard error increased substantially (Fig. 7 on the right), rendering all assay results not significantly different from the negative control. While some data points were comparable to Fig. 2, others were close to zero, indicating the particles could not aggregate. Either the components in human saliva or saline (NaCl) contributed to stabilizing the particles and facilitating them to induce antibody-antigen binding.

In summary, the SARS-CoV-2 monoclonal antibody to nucleocapsid proteins could distinguish omicron from delta variants and nucleocapsid from spike proteins. However, such distinction could not be found with the monoclonal antibody to spike proteins. The manufacturer reported the cross-reactivity of both types of antibodies to all SARS-CoV-2 variants. Therefore, these results may be unique to the current assay platform — the smartphone-based fluorescence microscope counting of particle immunoagglutination on a paper microfluidic chip platform. This result may suggest a clue to the role of nucleocapsid proteins in recognizing different variants.

Funding This work was supported by the Technology and Research Initiative Fund (TRIF) of the Arizona Board of Regents (ABOR).

Declarations

Conflict of interest The authors declare no competing interests.

References

1. WHO, Tracking the SARS-CoV-2 variants (last updated 19 July 2022). WHO. 2022. https://www.who.int/activities/tracking-SARS-CoV-2-variants. Accessed 25 July 2022.
2. Tanne JH. COVID-19: BA.5 variant is now dominant in US as infections rise. BMJ. 2022;378:o1770. https://doi.org/10.1136/bmj.o1770
3. Du Z, Hong H, Wang S, Ma L, Liu C, Bai Y, Adam DC, Tian L, Wang L, Lau EHY, Cowling BJ. Reproduction number of the omicron variant triples that of the delta variant. Viruses. 2022;14:821. https://doi.org/10.3390/v14040821.
4. Piri A, Kim HR, Park DH, Hwang J. Increased survivability of coronavirus and H1N1 influenza virus under electrostatic aerosol-to-hydrosol sampling. J Hazard Mater. 2021;2021(413): 125417. https://doi.org/10.1016/j.jhazmat.2021.125417.
5. Su X, Sutarlie L, Loh XJ. Sensors and analytical technologies for air quality: particulate matters and bioaerosols. Chem Asian J. 2020;15:4241–55. https://doi.org/10.1002/asia.202001051.
6. Rao A, Bassit L, Lin J, Verma K, Bowers HB, Pachura K, Greenleaf M, Sullivan J, Lai E, Creager RS, Martin GS, Lam WA. 2022. Assessment of the Abbott BinaxNOW SARS-CoV-2 rapid antigen test against viral variants of concern. iScience 2022;25:103968. https://doi.org/10.1016/j.isci.2022.103968
7. Ducharme J. Why the rise of rapid tests makes COVID-19 case counts hard to trust. Time 2022; April 21. https://time.

com/6168809/at-home-covid-19-test-results-should-i-report/. Accessed 25 July 2022.
8. Breshears LE, Nguyen BT, Akarapipad P, Sosnowski K, Kaarj K, Quirk G, Uhrlaub JL, Nikolich-Žugich J, Worobey M, Yoon JY. Sensitive, smartphone-based SARS-CoV-2 detection from clinical saline gargle samples. PNAS Nexus 2022;1:pgac028. https://doi.org/10.1093/pnasnexus/pgac028
9. Fabiani L, Mazzaracchio V, Moscone D, Fillo S, De Santis R, Monte A, Amatore D, Lista F, Arduini F. Paper-based immunoassay based on 96-well wax-printed paper plate combined with magnetic beads and colorimetric smartphone-assisted measure for reliable detection of SARS-CoV-2 in saliva. Biosens Bioelectron. 2022;200: 113909. https://doi.org/10.1016/j.bios.2021.113909.
10. Chung S, Breshears LE, Gonzales A, Jennings CM, Morrison CM, Betancourt WQ, Reynolds KA, Yoon JY. Norovirus detection in water samples at the level of single virus copies per microliter using a smartphone-based fluorescence microscope. Nat Protoc. 2021;16:1452–75. https://doi.org/10.1038/s41596-020-00460-7.
11. Akarapipad P, Kaarj K, Breshears LE, Sosnowski K, Baker J, Nguyen BT, Eades C, Uhrlaub JL, Quirk G, Nikolich-Žugich J, Worobey M, Yoon JY. Smartphone-based sensitive detection of SARS-CoV-2 from saline gargle samples via flow profile analysis on a paper microfluidic chip. Biosens Bioelectron. 2022;207: 114192. https://doi.org/10.1016/j.bios.2022.114192.
12. Suomalainen M, Liljestrom P, Garoff H. Spike protein-nucleocapsid interactions drive the budding of alphaviruses. J Virol. 1992;66:4737–47. https://doi.org/10.1128/jvi.66.8.4737-4747.1992.
13. Han P, Li L, Liu S, Wang Q, Zhang D, Xu Z, Han P, Li X, Peng Q, Su C, Gao GF, Wang P. Receptor binding and complex structures of human ACE2 to spike RBD from omicron and delta SARS-CoV-2. Cell. 2022;185:630–40. https://doi.org/10.1016/j.cell.2022.01.001.
14. Ye Q, Lu S, Corbett KD. Structural basis for SARS-CoV-2 nucleocapsid protein recognition by single-domain antibodies. Front Immunol. 2021;12: 719037. https://doi.org/10.3389/fimmu.2021.719037.
15. Sino Biological. SARS-CoV-2 (2019-nCoV) spike neutralizing antibody, mouse MAb. Sino Biological. 2022. https://www.sinobiological.com/antibodies/cov-spike-40591-mm48. Accessed 25 July 2022.
16. Sino Biological. SARS-CoV/SARS-CoV-2 nucleocapsid antibody, mouse MAb. Sino Biological. 2022. https://www.sinobiological.com/antibodies/cov-nucleocapsid-40143-mm05. Accessed 25 July 2022.

Sangsik Kim is currently working at the University of Arizona as a postdoctoral research associate. He is working on handheld sensor devices for environmental and biomedical applications.

Ciara Eades is an undergraduate student at the University of Arizona majoring in biochemistry. She is currently pursuing her career in the biochemistry field.

Jeong-Yeol Yoon is Professor at the University of Arizona in the Departments of Biomedical Engineering, Biosystems Engineering, and Chemistry & Biochemistry. He has worked on smartphone-based biosensors. He was President of the Institute of Biological Engineering in 2015 and is currently the Editor-in-Chief of the Journal of Biological Engineering, Associate Editor of Biosensors and Bioelectronics, and editorial board member for several other journals.